

# Determining the Appropriate Amount of Anesthetic Gas Using DWT and EMD Combined with Neural Network

Mustafa Coşkun · Hüseyin Gürüler · Ayhan Istanbulu ·  
Musa Peker

Received: 10 August 2014 / Accepted: 25 November 2014 / Published online: 4 December 2014  
© Springer Science+Business Media New York 2014

**Abstract** The spectrum of EEG has been studied to predict the depth of anesthesia using variety of signal processing methods up to date. Those standard models have used the full spectrum of EEG signals together with the systolic-diastolic pressure and pulse values. As it is generally agreed today that the brain is in stable state and the delta-theta bands of the EEG spectrum remain active during anesthesia. Considering this background, two questions that motivates this paper. First, determining the amount of gas to be administered is whether feasible from the spectrum of EEG during the maintenance stage of surgical operations. Second, more specifically, the delta-theta bands of the EEG spectrum are whether sufficient alone for this aim. This research aims to answer these two questions together. Discrete wavelet transformation (DWT) and empirical mode decomposition (EMD) were applied to the EEG signals to extract delta-theta bands. The power density spectrum (PSD) values of target bands were presented as inputs to multi-layer perceptron (MLP) neural network (NN), which predicted the gas level. The present study has practical implications in terms of using less data, in an effective way and also saves time as well.

**Keywords** Anesthesia · Estimating anesthetic gas level · Artificial intelligence · Discrete wavelet transform · Empirical mode decomposition

## Introduction

Anesthetic effect applied on a patient, is expressed as depth of anesthesia. In surgical operations, screening the depth of anesthesia in a reliable and non-invasive way and knowing the amount of anesthetic chemicals to be given to the patient have great importance [1]. However, the depth of anesthesia may vary depending on patient's condition (age, weight, etc.) and anesthetic agents [2]. It is important to measure accurately anesthetic dose, which applied to the patient during operation. Additionally, a calibration error which may occur in the evaporator can also adversely affect anesthesia process. Therefore, anesthetic gas level should be monitored continuously.

Recently, many research about determining anesthesia dose level and depth of anesthesia have been done [3–5]. Initial research concerning the evaluation of the depth of anesthesia involve blood pressure, tearing and heart rate however, these autonomic responses mostly affected by the skeletal muscle activity [6]. Actually, EEG signals contain important clues related to brain activity [7], such as sleep stages [8] and provides significant information such as epileptic seizure [9, 10]. Because anesthetic agents affect the brain's cortex, monitoring brain activity using EEG recording is a suitable approach to determine the depth of anesthesia [11]. These clues can also be used in the vital area of determining the patient's depth of general anesthesia during surgical operations [12, 13].

For the determination of the level of anesthesia, many different EEG based scientific models have been proposed in recent years. Among these models, bispectral index (BIS) is the most preferred parameter in determining level of

---

This article is part of the Topical Collection on *Systems-Level Quality Improvement*

---

M. Coşkun · A. Istanbulu  
Department of Computer Engineering, Faculty of Engineering and  
Architecture, Balıkesir University, 10145 Cagis, Balıkesir, Turkey

H. Gürüler (✉)  
Department of Information Systems Engineering, Faculty of  
Technology, Mugla Sıtkı Kocman University, 48000 Kotecli, Mugla,  
Turkey  
e-mail: hguruler@mu.edu.tr

M. Peker  
Department of Information Technologies, Samandıra Vocational and  
Technical School, Istanbul, Turkey

anesthetic hypnotic depth during the surgery. BIS value is formed from signals belong to four different EEG electrodes on brow area. This index is one of the high-grade spectral analysis methods. It is obtained by analyzing the correlation of phase between the parts of the signal [14].

In the past few years, various EEG based scientific models have been proposed for the identification of anesthesia level. For instance, some EEG entropy values were used as a criterion of depth of anesthesia according to the opinion that EEG signals become more regular as the anesthetic depth rises [15–17]. Zikov et al. [18] suggested a wavelet-based anesthesia value in order to identify the depth of anesthesia (wavelet analysis of value for central nervous system monitoring, WAVCNS). Researchers compared this method with index value from the BIS monitor for reference, and have presented a high correlation value ( $r=0.969$ ). Also, compared to the BIS value, WAVCNS has a faster algorithm [18]. For the measurement of the depth of anesthesia, Ferenets et al. [19] used spectral entropy based on the regularity and complexity, approximation entropy, Higuchi fractal dimension and the Lempel-Ziv complexity by taking advantage of EEG signals and as a result, they have achieved a good performance. Lalitha et al. [20] took advantage of the chaotic features and neural network classifiers such as correlation dimension, Lyapunov exponent and Hurst exponent in the determination of the levels of anesthetic depth. EEG monitorization is used for many purposes. Among these, there is providing pharmacodynamic effect of the anesthetic medicine or central nervous system (CNS) improvement in real time [21]. Tosun and Güntürkün [22] developed a neuro-fuzzy system to determine depth of anesthesia during the maintenance of anesthesia and to estimate anesthetic gas level applied at that moment. Also Güntürkün [23] designed a neural network system in another study, for the same purpose. The results achieved with this systems were quite successful.

#### Problem definition and purpose of the study

During the operation, the depth of the anesthesia of a patient is determined by the experience of the anesthetist. An anesthetic dose level which is applied to the patient must be measured sensitively as anesthetic depth may change momentarily in surgeries [24]. This is required to avoid awareness of patient occurring due to inadequate levels of anesthesia. Otherwise, patient can sense the operation pain and reacts in no way. Intra-operative awareness may also cause undesirable physiological results [25, 26]. On the other hand, over dosage of anesthetic drug can cause lethal effects on patient. To minimize such problems, anesthetist needs a reliable system to monitor the appropriate anesthetic dose level. The other problem is a calibration defect that may be occur in vaporizer, may carry the anesthesia process to a critical condition. Therefore, the level of the anesthetic gas which is regulated manually and

is given to a patient must be measured continuously, for checking whether the anesthetic dose level applied to patient is correct or not.

The major concern of the study is finding the appropriate dosage of the anesthetic drug during surgery. Saraoglu and Edin [2] have developed e-nose system to estimate the anesthetic dose level. This system determines gas concentration based on steady-state responses of the sensors [27–29]. The authors of more recent studies [21–23] have used the full spectrum of EEG without differentiating the frequency bands. Furthermore, these studies were generally built on to estimate depth of anesthesia, instead of estimating appropriate amount of anesthetic gas. However, predicting the dosage of anesthetic drug may help anesthetist to sure the patient be in safe.

In this study, a new neural system, which shows to experts sevoflurane gas ratio should be applied, was designed. This research addresses the appropriate level of anesthetic gas estimation according to corresponding PSD values of delta and theta bands (0.5–8 Hz) of EEG signals. Although EEG signal has a wide frequency band (0.5–100 Hz), clinical research mostly utilized frequency bands between 0.5 and 30 Hz [30]. EEG spectrum is namely involving  $\delta$  (0.5–4 Hz),  $\theta$  (4–8 Hz),  $\alpha$  (8–13 Hz),  $\beta_1$  (13–30 Hz) and  $\beta_2$  (31–50 Hz). The basic principle is that while low frequencies (below 8 Hz) of EEG signals reveal the stable and sleep state of the brain, higher frequencies (above 8 Hz) show that the brain is in an active state. In surgical operations, the increase of the amplitude of EEG wave below 8 Hz recorded from human brain under anesthesia shows a similar EEG mechanism to the sleep state of brain [31].

DWT and EMD were utilized to get the decomposition of non-stationary EEG signals is to uncover the delta-theta bands. Since the characteristics of the EEG waves are rather complex and the data sets in this study are constituted of large sizes, a MLP network was used as a classifier. The evidence from these studies suggest that PSD values of delta and theta bands of EEG signals are sufficient alone to predict gas ratio to maintain an appropriate anesthesia level.

The paper is organized as follows: Section “[Background](#)” provides information about the methods used in this study. Section “[Anesthesia data set](#)” gives brief information about the data set used in the study. Section “[Application methods and discussion](#)” presents information related to the implementation and evaluation step. The paper concludes with a brief discussion of the system that estimate the amount of anesthetic gas level in surgical operations using EEG signals.

#### Background

Records obtained from the patients under anesthesia are usually consists of long and noisy data. Therefore, systems which

are designed on these parameters cannot give adequately useful results. At this point, the request is emerging to operate in frequency band.

PSD is frequency response of a periodic or random signal. PSD indicates distribution of signal strength depending on the frequency and frequencies at which signal strength become intense [32, 33]. Power spectral density can be expressed with Eq. 1;

$$P_{PSD}(k) = \frac{1}{M} \sum_{i=1}^M |x_i(k)|^2 \tag{1}$$

where  $M$  is the number of samples,  $x$  is signal,  $x_i(k)$  represents the Fourier transform of the  $x$  signal.  $x_i(k)$  is calculated as shown in Eq. 2.

$$x_i(k) = \sum_{n=0}^{N-1} x_i(n) e^{-j\frac{2\pi}{N}nk} \tag{2}$$

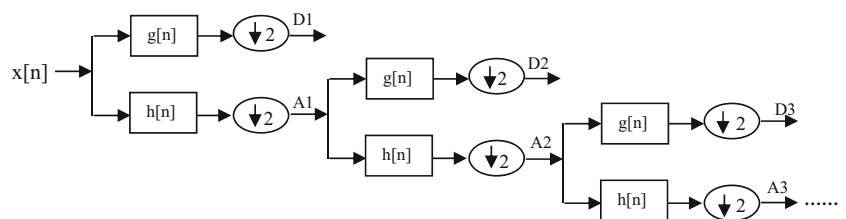
Since EEG signals are non-stationary, both DWT and EMD are capable of display the energy of the signals in time-frequency space [34]. DWT has been employed in many applications concerning EEG data analysis [35], since it is a more advanced method with improved algorithms for the processing of non-stationary signal compared to the existing methods such as FFT analysis. EMD is a new approach, which eliminates the requirement for the stationary of signals.

### Discrete Wavelet Transformation (DWT)

DWT is effective in presenting an opportunity to allow the decomposition of a signal into a number of scales and wavelets, which are associated with low, and high pass filters [36]. Figure 1 shows the sub band coding of DWT decomposition of the original signal ( $x[n]$ ).

Here,  $g[n]$  is a high pass filter used to discrete original signal and gives the detail D1, on the other side  $h[n]$  is a low pass filter and provides the approximation A1. The details are the low-scale and high frequency components, whereas the approximations are the high-scale and low frequency components of the original signals [37]. The approximations are found after the first decomposition. The DWT decomposition process can be easily repeated to achieve further decompositions by using the approximations as shown in Fig. 1 [38].

**Fig. 1** Subband decomposition of the DWT implementation



The outputs of the high and the low pass filters can be defined as:

$$y_{high}[k] = \sum_n x[n].g[2k-n] \tag{3}$$

$$y_{low}[k] = \sum_n x[n].h[2k-n] \tag{4}$$

### Empirical Mode Decomposition (EMD)

The purpose of EMD is to empirically separate a signal into several sub-signals of variation and frequency content [39]. Since they are empirically derived from the data, sub-signals are referred to as intrinsic mode functions (IMFs) used to decompose a time series into finite numbers and their summation produces the original signal. Each of the IMFs, linear or nonlinear, plays a role as a simple oscillation, which has the same number of extremes and zero-crossings [34]. Determining the IMFs, frequency components of a signal, using many filters is thought to give valuable information about the signal [39]. Also, a practical way of shifting data is used to generate IMFs, which have the same numbers of zero crossings and extremes [34]. The algorithm used to create IMFs in the EMD is obtained in two main steps:

Step-1: Identify all the local extreme points of the original signals in the experimental data  $x(t)$ .

The mean of upper and lower envelopes of data  $x(t)$  is calculate as Eq. 5:

$$m_1(t) = \frac{U(t) + L(t)}{2} \tag{5}$$

where  $U(t)$  refers to the upper envelope of data and  $L(t)$  refers to the lower envelope of data.

$$h_1(t) = x(t) - m_1(t) \tag{6}$$

The resulting component  $h(t)$  is an IMF that is symmetric and satisfies all the maxima positive and all the minima negative. If this is not the result then the separating process will be repeated until the extracted signal is in an IMF format.

$$h_{11}(t) = h_1(t) - m_{11}(t) \tag{7}$$

Step-2:

$$r_1(t) = x(t) - c_1(t) \tag{8}$$

The first IMF is subtracted from the original signal and the equation  $c_1 = h_1(t)$  is applied and  $r_1(t)$  is the residue. By applying the procedures of *step-1* and *step-2*, more intrinsic modes are observed until the final one, which represents the general trend of the time series.

$$x(t) = \sum_{i=1}^n c_i(t) + r_n \tag{9}$$

$$r_{i-1}(t) - c_i(t) = r_i(t) \tag{10}$$

MLP neural network

The NN is a nonparametric technique for performing a wide variety of detection and estimation tasks due to the ability to find nonlinear surfaces separating the underlying patterns [40]. A MLP network use the steepest descent method to update the weights during the training period and all the layers use non-linear sigmoid activation functions. The weights between layers ( $i$ ) and neurons ( $j$ ) are updated as:

$$W_{ji}(t + 1) = \Delta W_{ji}(t) + c\delta_j x_i \tag{11}$$

where  $c$  is the learning coefficient,  $\delta_j$  is the local gradient which is a term given to the hidden or output layer of any neuron. For the output layer;

$$\delta_j = \frac{\partial f}{\partial net_j} (y_j^{(t)} - y_j) \tag{12}$$

in which  $net_j = \sum x_j w_{ji}$  and  $y_j^{(t)}$  refers to the desired output of  $j$  neuron. When the hidden and input layer is considered, the situation can be represented as:

$$\delta_j = \left( \frac{\partial f}{\partial net_j} \right) \sum w_{ji} \delta_j \tag{13}$$

Since any number of  $y_j^{(t)}$  can exist starting from the first iteration, steepest descent method searches the reverse side of gradient in order to find the local minimums [41]. So, the optimal weights ensuring minimum error can be acquired along the current line.

Anesthesia data set

In this study, EEG data was recorded with a 22-channel EEG device with a 500 Hz sampling frequency. An international 8-channel bipolar 10-20-montage system was utilized to collect patient data. To obtain a normal level the patient’s EEG waves were recorded before the sevoflurane gas was administered by the anesthesiologist.

Sevoflurane is a sweet-smelling, nonflammable, highly fluorinated methyl isopropyl ether used for induction and maintenance of general anesthesia. Since sevoflurane has an excellent safety record, particularly for outpatient anesthesia, it is one of the most commonly used volatile anesthetic agents [42].

The sample group of patients (see Table 1) had been admitted to Kutahya Hospital, Turkey. The surgical applications were basic operations such as hernia and lasted approximately 1 h. The data sets each contains a 30-s section of the EEG signals collected from ten different patients.

Application methods and discussion

Pre-processing

A pre-processing procedure was applied to eliminate undesired noisy signals from the original EEG for all the data sets. Since this research focuses on low frequency bands, a 30Hz 10th order Infinite Impulse Response (IIR) type low pass Butterworth filter was utilized to eliminate noisy signals related to high frequencies [30].

Time-frequency analysis

The purpose of differentiating the EEG signals into several sub-signals is to obtain the purer delta-theta bands. The study analyzes the time-frequency of each EEG signal

**Table 1** The information of the anesthesia data set

Patient	Gender (F/M)	Age	Operation type
1	F	65	Appendicitis
2	F	60	Thyroidectomy
3	F	60	Cholecystectomy
4	F	58	Cholecystectomy
5	F	55	Appendicitis
6	F	52	Thyroidectomy
7	F	45	Cholecystectomy
8	M	60	Hernia
9	M	59	Hernia
10	M	55	Appendicitis

using two different techniques DWT and EMD. These two techniques were separately implemented to the pre-processed EEG signals to extract delta-theta bands. Figure 2 shows all the process undertaken to estimate the amount of gas to be administered through a flow chart. The flow chart involves the processes with the proposed methods, DWT and EMD combined with MLP neural networks.

*Time-frequency analysis with DWT*

In this study, non-stationary EEG signals are decomposed into subbands using DWT with the Daubechies wavelet of order 2 (db-2). Because it had the best performance in the classification of the EEG segments using a symmetric-padding mode. We empirically found that the 3rd level decomposition of EEG bands was positively related to the level of anesthesia. Figure 3 shows the PSD values of the EEG signal after 3rd level decomposition (approximations and details).

Essentially, approximations are purified EEG signals and reflect the efficiency of the Daubechies wavelet. As shown in Fig. 3a, they also reveal the delta-theta bands coverage, thus it

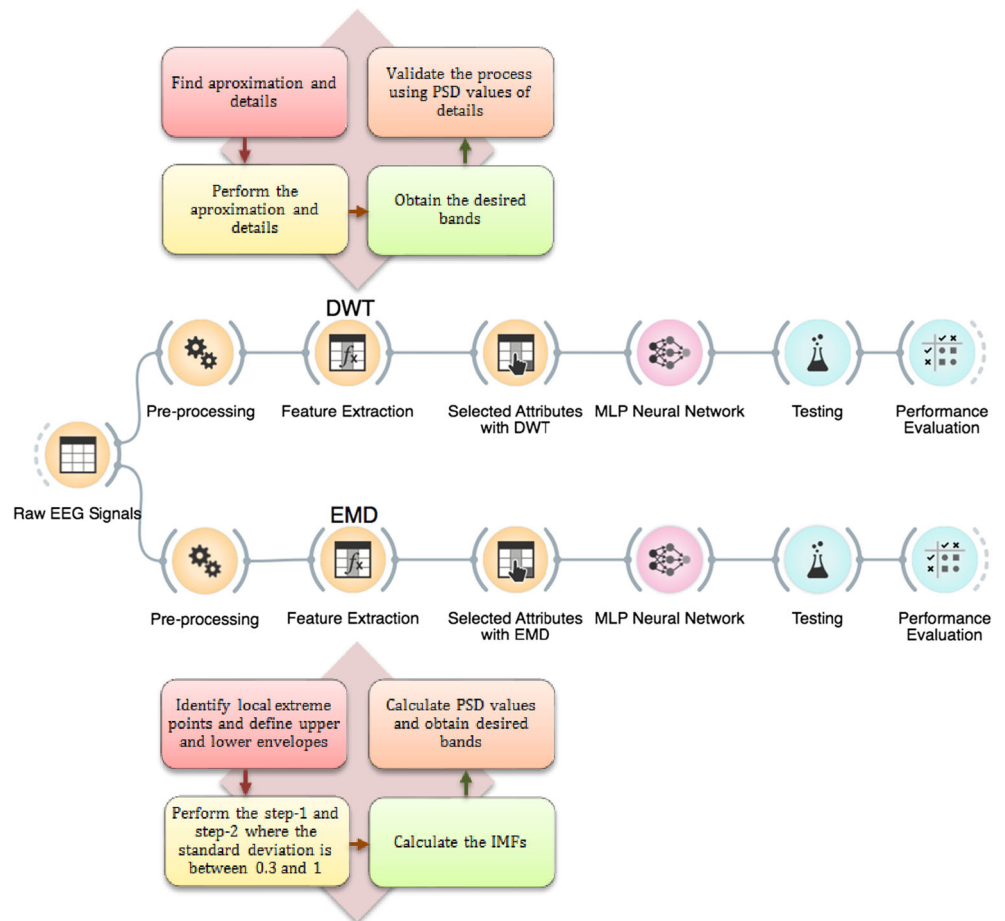
can also allow to obtain the delta-theta bands of the EEG spectrum. Whereas, Fig. 3b shows that the PSD values of undesired signals reach maximum values in the delta-theta bands, which means that noisy signals effects are minimized around related bands.

*Time-frequency analysis with EMD*

The tests for differentiating the EEG signals into several sub-signals were performed with 1st and 2nd degrees of EMD functions. 2nd degree IMFs were also applied to pre-processed EEG signals. Figure 4 shows the PSD values of the IMFs.

As shown in Fig. 4, the PSD values of 2nd degree IMFs only cover the delta-theta bands and the efficiency of the maximum values was around 2–8 Hz as expected. Whereas the PSD values of 1st degree IMFs overlap the alpha bands. However, the alpha band is sign of awakening and indicates that the brain is changing its stability. Therefore, the PSD values of the 2nd degree IMFs that represent the requested bands have been obtained. The desired frequency bands of the EEG signals were also efficiently evaluated by EMD.

**Fig. 2** A graphical illustration of the methodology employed in this study



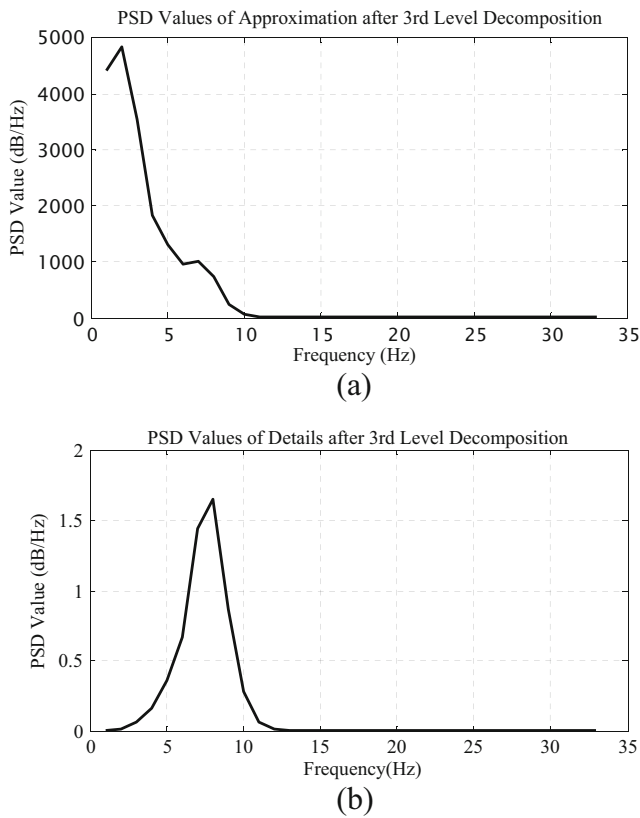


**Fig. 3** PSD values after 3rd level decomposition. **a** Approximations **b** Details

Neural application

In this study, the appropriate level of anesthetic gas to be administered was estimated according to corresponding PSD values of current EEG signals, which were obtained after DWT and EMD analysis presented as an input to the MLP network. As a requirement of supervised learning, previous anesthetic gas levels applied by the anesthesiologist were also presented as an input the MLP network.

The network typology was a feed-forward structure with back-propagation algorithm consisting of 20 input layer neurons, 15 hidden layer neurons and an output layer neuron. The

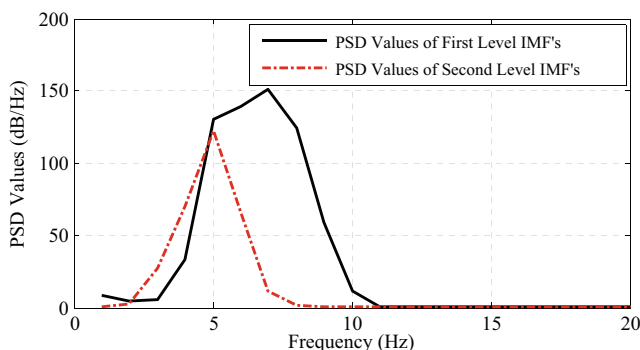


**Fig. 4** PSD values of the IMFs

data sets were divided into training and test groups as a requirement of supervised learning. This MLP network was use the steepest descent method to update the weights during the training period and all the layers use non-linear sigmoid activation functions.

In supervised learning, we are given a set of example pairs  $(x, y), x \in X, y \in Y$  and the aim is to find a function  $f : X \rightarrow Y$  in the allowed class of functions that matches the examples. In other words, we wish to infer the mapping implied by the data; the cost function is related to the mismatch between our mapping and the data and it implicitly contains prior knowledge about the problem domain.

A commonly used cost is the mean-squared error, which tries to minimize the average squared error between the network's output,  $f(x)$ , and the target value  $y$  over all the example pairs. When one tries to minimize this cost using gradient descent for the class of neural networks called multilayer perceptron, one obtains the common and well-known back propagation algorithm for training neural networks [43]. Figure 5 shows an artificial neuron model.

A log-sigmoid function, also known as a logistic function, is given by the relationship Eq. 14;

$$\sigma(t) = \frac{1}{1 + e^{-\beta t}} \tag{14}$$

where  $\beta$  is a slope parameter. Sigmoid functions in this respect are very similar to the input–output relationships of biological neurons, although not exactly the same.

Table 2 shows the NN training parameters.

Figure 6 shows the structure of the NN. The first selected 19 PSD values of 30-s EEG records were used as the inputs of the 3-layer feed-forward network since they carried meaningful values. The number of input layer nodes is equal to the total number of PSD values and the previous anesthesia rate. Similarly, the number of output layer nodes is the same as the number of output. The number of hidden layer node is less than nodes of the input layer and this is in order to sustain network simplicity.

The optimum network design that was realized fulfilled the minimum requirements of the MLP inputs with the maximum

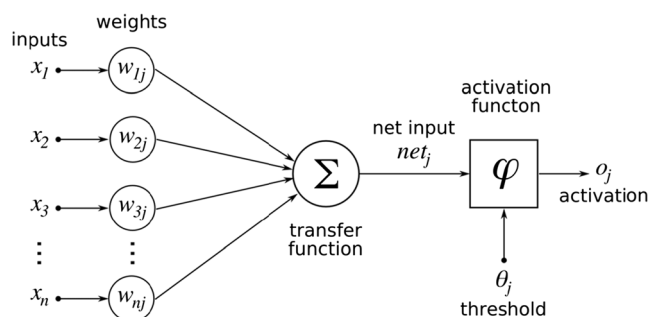


**Fig. 5** Artificial neuron model [43]

**Table 2** MLP NN training parameters

Training parameters	Values
Activation function	Logarithmic sigmoid
Initial learning rate	0.8
Performance type	(MSE)
Number of layers	3
Input layer of MLP	20
Hidden layer of MLP	15
Output layer of MLP	1
Momentum constant	0.9

effect. Therefore, the PSD values of each data set were selected rather than using the signal itself in order to decrease the complexity of the MLP network and allow an appropriate network structure to be drawn. A basic outline of the MLP network designed in this study consisted of three layers (20 input layer neurons, 15 hidden layer neurons and an output layer neuron) as shown in Fig. 6. The first 19 PSD values of the EEG records were used and remaining PSD values were ignored due to the fact that they were converging to zero values. To determine the PSD values of 30-s EEG records, the average EEG values were taken from the patient, were calculated for the 5 min before anesthesia and during the maintenance stage. This gave the MLP network the opportunity to tolerate unexpected inputs or find a way to avoid an extensive training period for every significant deviation. The first 19 PSD values of EEG signals and the previous anesthetic gas levels were presented as the inputs of MLP. Here, the anesthetic gas ratio applied by the anesthesiologist was used as the criteria for updating weights of the network. This is in keeping with the supervised method that supports the learning process to obtain the best prediction of the applied gas amount for new cases.

Root Mean Square Error (RMSE) was used to determine the error ratio between the administered gas level and the

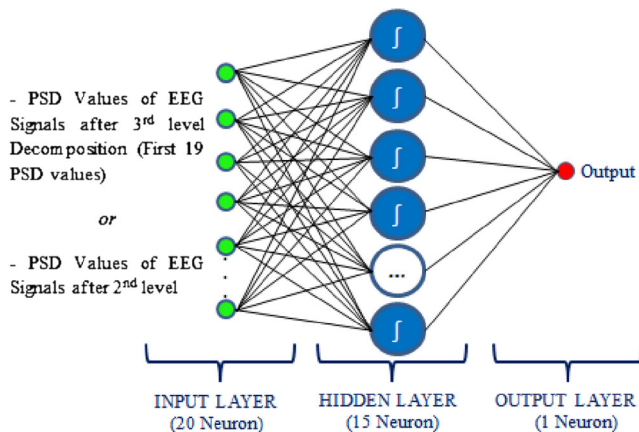


**Fig. 6** Multi-layer perceptron network structure

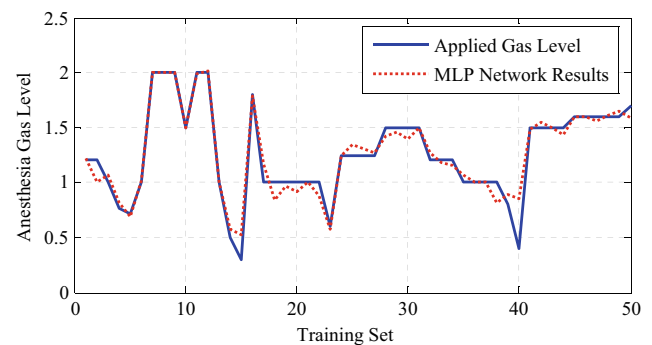
predicted ones [44]. Eq. 15 gives the RMSE definition.

$$RMSE = \sqrt{\frac{\sum_{i=1}^n (y_a - y_p)^2}{n}} \tag{15}$$

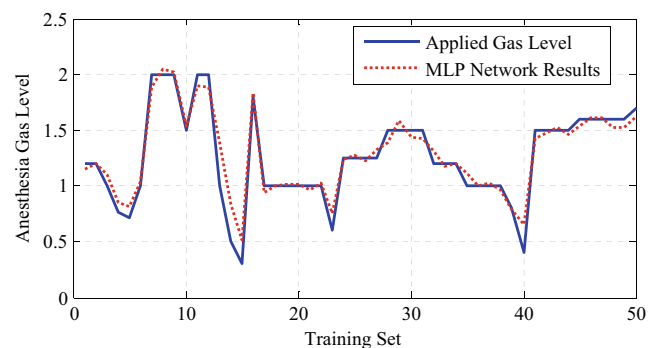
Where  $y_a$  is the gas level applied by the anesthesiologist and  $y_p$  is the gas level predicted by the system. The amount of the error is, therefore,  $\epsilon = (y_a - y_p)$ . When the RMSE approaches zero, this gives the predicted value higher percentage accuracy.

Figure 7 shows MLP NN training results using DWT, and EMD. The solid line shows that gas level administered by the anesthesiologist and the dotted line shows the MLP NN results for DWT or EMD.

Although some similar results can be obtained by the use of less complex MLP architectures, as the number of neurons in the layers decreases, the learning is getting slower and sometimes comes to a fixed error rate. Moreover, MLP Network sometimes memorizes the results to applied gas ratio rather than generalize with less neuron. Since the paper aims to obtain optimum number of neurons 20-15-1 network architecture were preferred and 15 neurons for hidden layer was found the most favorable. Tables 3 and 4 show complexity analysis for sevoflurane gas ratio estimations of MLP Networks both DWT and EMD.



(a)



(b)

**Fig. 7** The training results from the MLP NNs **a** Training results for DWT. **b** Training results for EMD

**Table 3** Complexity analysis of MLP networks with DWT

Number	Sevoflurane gas level actually applied by an anesthesiologist (%)	Test set results with DWT					
		Input layer: 20 hidden layer:5		Input layer: 20 hidden layer:10		Input layer: 20 hidden layer:15	
		Estimated results obtained using the DWT based neural system (%)	$\varepsilon_{DWT(n)}^2$	Estimated results obtained using the DWT based neural system (%)	$\varepsilon_{DWT(n)}^2$	Estimated results obtained using the DWT based neural system (%)	$\varepsilon_{DWT(n)}^2$
1	1.5	1.08	0.1764	1.62	0.0144	1.58	0.0064
2	1.25	1.15	0.0100	1.11	0.0196	1.24	0.0001
3	1.25	1.14	0.0121	1.19	0.0036	1.28	0.0009
4	1.2	1.06	0.0196	1.15	0.0025	1.16	0.0016
5	1	1.08	0.0064	1.06	0.0036	0.88	0.0144
6	1.5	1.14	0.1296	1.29	0.0441	1.40	0.01
7	1.5	1.18	0.1024	1.58	0.0064	1.42	0.0064
8	1.7	1.50	0.0400	1.63	0.0049	1.64	0.0036
9	1.7	2.24	0.2916	1.84	0.0196	1.59	0.0121
10	1.7	1.74	0.0016	1.72	0.0004	1.62	0.0064
<i>RMSE<sub>DWT</sub></i>		0.2810		0.1091		0.0787	

The MLP network training period was stopped after 2200 iterations for both methods in order to compare results with each other. As shown Fig. 7 that minor differences occurred during the training periods and the errors for the two methods were observed to be very low. The lower errors implies a higher prediction capacity. Fundamentally, EMD is an empirical method and only learns using iterations in contrast to DWT. The test results shown in Tables 3 and 4 reveal that the neural network reached an RMSE accuracy levels of 0.0787 for DWT and

0.0693 for EMD according to amount of anesthesia gas administered.

In Tables 3 and 4, sevoflurane gas level actually applied by an anesthesiologist exists in the first row, whereas the results from MLP based network structures take place in the second row. Successful results were obtained with both test sets in the estimation of the gas level at the maintenance phase of anesthesia. According to the average relative percentage error calculation, success rate of network trained with DWT is 94.95 %, success rate of network trained with EMD is

**Table 4** Complexity analysis of MLP networks with EMD

Number	Sevoflurane gas level actually applied by an anesthesiologist (%)	Test set results with EMD					
		Input layer: 20 hidden layer:5		Input layer: 20 hidden layer:10		Input layer: 20 hidden layer:15	
		Estimated results obtained using the EMD based neural system (%)	$\varepsilon_{EMD(n)}^2$	Estimated results obtained using the EMD based neural system (%)	$\varepsilon_{EMD(n)}^2$	Estimated results obtained using the EMD based neural system (%)	$\varepsilon_{EMD(n)}^2$
1	1.5	1.74	0.0576	1.44	0.0036	1.46	0.0016
2	1.25	1.08	0.0289	1.34	0.0081	1.15	0.01
3	1.25	1.11	0.0196	1.29	0.0016	1.34	0.0081
4	1.2	0.91	0.0841	1.11	0.0081	1.23	0.0009
5	1	0.66	0.1156	0.98	0.0004	1.08	0.0064
6	1.5	0.86	0.4096	1.26	0.0576	1.42	0.0064
7	1.5	1.28	0.0484	1.37	0.0169	1.43	0.0049
8	1.7	1.53	0.0289	1.75	0.0025	1.64	0.0036
9	1.7	1.86	0.0256	1.69	0.0001	1.65	0.0025
10	1.7	1.54	0.0256	1.71	0.0001	1.64	0.0036
<i>RMSE<sub>EMD</sub></i>		0.2905		0.0995		0.0693	



95.16 %. The results show the capability of designing a new intelligent assistance for anesthetic agent scoring system. Despite the application of attributes obtained with different methods to the network structure, success rates are close to each other. Success rate is approximately 95 % for both methods. This shows the stability of the proposed system.

## Conclusions

This study estimates the appropriate level of anesthetic gas ratio according to corresponding PSD values of delta and theta bands (0.5–8 Hz) of EEG signals. Best of our knowledge, it is a new approach that a neural system suggests sevoflurane gas ratio to anesthesiologists for controlling anesthesia level at the maintenance stage of general anesthesia. We propose a system using a narrower frequency band, unlike recent studies use the full spectrum of EEG waves [21–23, 45, 46]. The results of the present study demonstrate that the delta and theta bands of the EEG spectrum where the brain is in stable state were sufficient alone to detect sevoflurane gas ratio. Therefore, the study, also, prove that the delta and theta bands of the EEG spectrum is related to anesthesia. Two time-frequency signal analysis methods, DWT and EMD, were utilized for each EEG to extract PSD values of the related bands. Experiments were performed under similar conditions such as the type and duration of the surgical operations, focusing on a specific age group and the same EEG recording process. For the limited numbers of PSD values obtained from DWT and EMD empirically provided to MLP network as inputs, the network typologies were designed in a simply way. The networks responded without using any medical measurements in addition to EEG signals as inputs such as diastolic pressure, systolic pressure and pulse. As a result, the network processed in a more effective way with fewer data/rules and the reduced a loss of time. The results obtained from the RSME of the two methods prove that the estimation of anesthetic gas level to be administered was generated by the system.

**Acknowledgments** We would like to thank Dr. Mustafa Tosun for supplying the patient data.

## References

- Gurkan, G., Cebeci, B., Demiralp, T. and Akan, A., Topographic and temporal spectral analysis of EEG signals during anaesthesia. *Biomedical Engineering Meeting (BIYOMUT)*. pp.1–4, 2010.
- Saraoglu, H. M., and Edin, B., E-Nose system for anesthetic dose level detection using artificial neural network. *J. Med. Syst.* 31(6): 475–482, 2007.
- Mahfouf, M., Asbury, A. J., and Likens, D. A., Unconstrained and constrained generalized predictive control of depth of anesthesia during surgery. *Control. Eng. Pract.* 11:1501–1515, 2003.
- Becker, K., Thull, B., Kasmacher-Leidinger, H., Stemmer, J., Rau, G., Kalf, G., and Zimmermann, H., Design and validation of an intelligent patient monitoring and alarm system based on fuzzy logic process model. *Artif. Intell. Med.* 11:33–53, 1997.
- Vefghi, L., and Linkens, D. A., Internal representation in neural networks used for classification of patient anesthetic states and dosage. *Comput. Methods Prog. Biomed.* 59:75–89, 1999.
- Huang, J. W., Lu, Y. Y., Nayak, A., and Roy, R. J., Depth of anesthesia estimation and control. *IEEE Trans. Biomed. Eng.* 46: 71–81, 1999.
- Bos, D.P.O., Duvinage, M., Oktay, O., Saa, J.D., Guruler, H. and Istanbul, A. et al., Looking around with your brain in a virtual world. *IEEE Symp. Comput. Intell. Cogn. Algorithms, Mind, Brain*, pp. 1–8, 2011.
- Fraivan, L., Lweesy, K., Khasawneh, N., Wenz, H., and Dickhaus, H., Automated sleep stage identification system based on time-frequency analysis of a single EEG channel and random forest classifier. *Comput. Methods Prog. Biomed.* 108:10–19, 2011.
- Pachori, R. B., and Bajaj, V., Analysis of normal and epileptic seizure EEG signals using empirical mode decomposition. *Comput. Methods Prog. Biomed.* 104:373–381, 2011.
- Päivinen, N., Lammi, S., Pitkänen, A., Nissinen, J., Penttonen, M., and Grönfors, T., Epileptic seizure detection: A nonlinear viewpoint. *Comput. Methods Prog. Biomed.* 79:151–159, 2005.
- Traast, H. S., and Kalkman, C. J., Electroencephalographic characteristics of emergence from propofol/sufentanil total intravenous anesthesia. *Anesth. Analg.* 81:336–371, 1995.
- Franks, N. P., General anaesthesia: From molecular targets to neuronal pathways of sleep and arousal. *Nature* 9:370–386, 2008.
- Al-Kadi, M. I., Reaz, M. B. I., and Ali, M. A. M., Evolution of electroencephalogram signal analysis techniques during anesthesia. *Sensors Basel Switzerland* 13:6605–6635, 2013.
- Zoughi, T., Boostani, R., and Deypir, M., A wavelet-based estimating depth of anesthesia. *Eng. Appl. Artif. Intell.* 25(8):1710–1722, 2012.
- Ferenets, R., et al., Comparison of entropy and complexity measures for the assessment of depth of sedation. *IEEE Trans. Biomed. Eng.* 53(6):1067–1077, 2006.
- Zhang, X. S., and Roy, R. J., Derived fuzzy knowledge model for estimating the depth of anesthesia. *IEEE Trans. Biomed. Eng.* 48: 312–323, 2001.
- Bruhn, J., Lehmann, L. E., Röpcke, H., Bouillon, T. W., and Hoeff, A., Shannon entropy applied to the measurement of the electroencephalographic effects of desflurane. *Anesthesiology* 95:30–35, 2001.
- Zikov, T., Bibian, S., Dumont, G. A., Huzmezan, M., and Ries, C. R., Quantifying cortical activity during general anesthesia using wavelet analysis. *IEEE Trans. Biomed. Eng.* 53(4):617–632, 2006.
- Ferenets, R., Lipping, T., Suominen, P., Turunen, J., Puumala, P., Jantti, V., Himanen, S. L., and Huotari, A. M., Comparison of the properties of EEG spindles in sleep and propofol anesthesia. *IEEE Eng. Med. Biol. Soc.* 1:6356–6359, 2006.
- Lalitha, V., and Eswaran, C., Automated detection of anesthetic depth levels using chaotic features with artificial neural networks. *J. Med. Syst.* 31(6):445–452, 2007.
- Tosun, M., Ferikoglu, A., Gunturkun, R., and Unal, C., Control of sevoflurane anesthetic agent via neural network using electroencephalogram signals during anesthesia. *J. Med. Syst.* 36:451–456, 2012.
- Tosun, M., and Gunturkun, R., Anesthetic gas control with neuro-fuzzy system in anesthesia. *Expert Syst. Appl.* 37(3):2690–2695, 2010.
- Gunturkun, R., Estimation of medicine amount used anesthesia by an artificial neural network. *J. Med. Syst.* 34(5):941–946, 2010.
- Sleigh, J. W., Andrzejowski, J., Steyn-Ross, A., et al., The bispectral index: A measure of depth of sleep? *Anesth. Analg.* 88:659–661, 1999.

25. Nahm, W., Stockmanns, G., Petersen, J., Gehring, H., Konecny, E., Kochs, H. D., and Kochs, E., Concept for an intelligent anaesthesia EEG monitor. *Med. Inform. Internet. Med.* 24(1):1–9, 1999.
26. Moerman, N., Bonke, B., and Oosting, J., Awareness and recall during general anesthesia: Facts and feelings. *Anesthesiology* 79:454–464, 1993.
27. Temurtas, F., Tasaltin, C., Temurtas, H., Yumusak, N., and Ozturk, Z. Z., Fuzzy logic and neural network applications on the gas sensor data: concentration estimation. *Lect. Notes Comput. Sci* 2869:179–186, 2003.
28. Gulbag, A., and Temurtas, F., A study on quantitative classification of binary gas mixture using neural networks and adaptive neuro fuzzy inference systems. *Sens. Actuators B* 115:252–262, 2006.
29. Yusubov, I., Gulbag, A., and Temurtas, F., A study on mixture classification using neural network. *Electr. Lett. Sci. Eng.* 3(1):44–49, 2007.
30. Adeli, H., Zhou, Z., and Dadmehr, N., Analysis of EEG records in an epileptic patient using wavelet transform. *J. Neurosci. Methods* 123: 69–87, 2003.
31. Soo-young Ye, G. J., et al., Development for the evaluation index of an anesthesia depth using the bispectrum analysis. *Int. J. Biol. Med. Sci.* 4:67–70, 2009.
32. Chongsheng, L., Study of weak signal detection based on second FFT and chaotic oscillator. *Nat. Sci.* 3(2):59–64, 2005.
33. Ustundag, M., Sengur, A., Gokbulut, M., and Ata, F., Weak signal detection algorithm based on Fourier transform, 6th International Advanced Technologies Symposium (IATS'11), pp.97–100, 2011.
34. Wu, M., and Huang, N. E., Biomedical data processing using HHT: A review, in: A. Nait-Ali (Ed.), *Adv. Biosignal Process.*, Springer Berlin Heidelberg, pp. 335–352, 2009.
35. Prochazka, A., Kukal, and J. Vysata, O., Wavelet transform use for feature extraction and EEG signal segments classification. *3rd Int. Symp. Commun. Control Signal Process.* pp. 719–72, 2008.
36. Sen, B., and Peker, M., Novel approaches for automated epileptic diagnosis using FCBF feature selection and classification algorithms. *Turk J Electr Eng Comput Sci* 21:2092–2109, 2013.
37. Sen, B., Peker, M., Celebi, F. V., and Cavusoglu, A., A comparative study on classification of sleep stage based on EEG signals using feature selection and classification algorithms. *J. Med. Syst.* 38(3):1–21, 2014.
38. Tawade, L., and Warpe, H., Detection of epilepsy disorder using discrete wavelet transforms using MATLABs. *Int. J. Adv. Sci. Technol.* 28:17–24, 2011.
39. Battista, B. M., Knapp, C., McGee, T., and Goebel, V., Application of the empirical mode decomposition and Hilbert-Huang transform to seismic reflection data. *Geophysics* 72:H29–H37, 2007.
40. Haykin, S., *Neural Networks: A Comprehensive Foundation*, Prentice Hall, 1999.
41. Sheikhtaheri, A., Sadoughi, F., and Hashemi Dehaghi, Z., Developing and using expert systems and neural networks in medicine: A review on benefits and challenges. *J. Med. Syst.* 38(9):1–6, 2014.
42. U.S. National Library of Medicine, Livertox: Clinical and Research Information on Drug-Induced Liver Injury (2014), Drug Record: Sevoflurane (Accessed 15.08.2014)
43. Artificial Neural Network, [http://en.wikipedia.org/wiki/Artificial\\_neural\\_network](http://en.wikipedia.org/wiki/Artificial_neural_network) (Accessed: 10.11.2014)
44. Cakir, A., and Demirel, B., A software tool for determination of breast cancer treatment methods using data mining approach. *J. Med. Syst.* 35:1503–1511, 2010.
45. Güntürkün, R., Using Elman recurrent neural networks with conjugate gradient algorithm in determining the anesthetic the amount of anesthetic medicine to be applied. *J. Med. Syst.* 34(4):479–484, 2010.
46. Saraoğlu, H. M., and Şanlı, S., A fuzzy logic-based decision support system on anesthetic depth control for helping anesthetists in surgeries. *J. Med. Syst.* 31(6):511–519, 2007.